

# Rate limiting steps of the phase transformations in Ti-doped NaAlH<sub>4</sub> investigated by isotope exchange

W. Lohstroh\* and M. Fichtner

*Institute of Nanotechnology, Forschungszentrum Karlsruhe, Postfach 3640, 76021 Karlsruhe, Germany*

(Received 28 October 2006; revised manuscript received 5 January 2007; published 15 May 2007)

The sorption kinetics of Ti-doped NaAlH<sub>4</sub> has been investigated under the aspect of the replacement of hydrogen by deuterium. For both desorption and absorption, kinetics is found to be slower in the deuterated than in the protonated samples. Comparison of the apparent activation energies and the prefactors indicates that a hydrogen-containing species heavier than H determines the reaction rate.

DOI: 10.1103/PhysRevB.75.184106

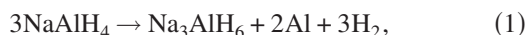
PACS number(s): 82.30.-b, 82.20.Tr, 66.30.Pa

## I. INTRODUCTION

A future hydrogen economy requires safe, reliable, and efficient hydrogen-storage facilities to be developed. A solid hydrogen-storage material would be an ideal solution; however, classical hydrides with typical hydrogen contents of ~1.5 wt % lack the capacity required for mobile applications. Since the discovery by Bogdanović and Schwickardi<sup>1</sup> that NaAlH<sub>4</sub> mixed with a Ti-based additive can reversibly release and store hydrogen, complex hydrides have been considered as promising storage materials, with numerous studies being devoted to their sorption properties.<sup>2-4</sup> Ti-doped NaAlH<sub>4</sub> reversibly releases and stores approximately 4 wt % hydrogen at operating temperatures of 100–150 °C.<sup>2</sup> So far, this reversible storage capacity at this temperature level is unique among the complex hydrides although various efforts have been made to access higher capacity hydrides, e.g., LiBH<sub>4</sub>,<sup>5</sup> Li<sub>4</sub>BN<sub>3</sub>H<sub>10</sub>,<sup>6-8</sup> or mixtures of complex hydrides and binary hydrides<sup>9</sup> for reversible storage.

In NaAlH<sub>4</sub>, the addition of Ti-based additives has an exceptional effect on the reversibility and reaction speed of both the decomposition and reabsorption reactions. However, the underlying mechanism is not well understood. A classical catalytic effect, i.e., Ti promoting the dissociation and recombination of hydrogen molecules, has been ruled out.<sup>3,10</sup> Several studies conclude that the decomposition reaction of alanates can be described in a nucleation and growth model which is diffusion limited,<sup>3,11-13</sup> although the nature of the diffusing species has not yet been clarified. Hydrogen diffusion through the lattice could be a possibility, though it seems unlikely that this is the rate-controlling step in a solid-state reaction involving mass transport on a major scale. Another reaction mechanism is proposed which provides highly mobile Al in the form of AlH<sub>3</sub>.<sup>14</sup> Recently, molecular aluminum hydrides have been identified in Ti-doped NaAlH<sub>4</sub> by inelastic neutron scattering.<sup>15</sup> In order to clarify the nature of the rate limiting reaction step, the authors investigated the hydrogen uptake and release of NaAlH<sub>4</sub> doped with Ti clusters with respect to the replacement of hydrogen by deuterium. Comparison of the kinetics displayed by the two isotopes provides insight into the exceptional sorption properties of Ti-doped NaAlH<sub>4</sub>.

The decomposition of NaAlH<sub>4</sub> occurs in two steps:



The first and second decomposition steps release 3.7 and 1.85 wt % hydrogen, respectively. In a third step, the decomposition of NaH yields another 1.85 wt % although the necessary temperature in this case is above 400 °C, which is considered too high for practical application.

This paper is about the isotope effect of hydrogen release and uptake in Ti-doped NaAlH<sub>4</sub>. A series of kinetic measurements have been conducted for both the protonated and deuterated cases. The apparent activation energies and the prefactors will be compared and discussed below.

## II. EXPERIMENT

As-received NaAlH<sub>4</sub> (Albemarle 96%) mixed with 5 mol % Ti [on the basis of colloidal Ti<sub>13</sub>·6THF (THF: tetrahydrofuran)] was ball milled for 30 min (ball-to-powder ratio 20:1, 600 rpm) in a Si<sub>3</sub>N<sub>4</sub> vial. The powder was handled in a glovebox in a purified Ar atmosphere in order to minimize exposure to oxygen and moisture. Details of the sample preparation and the preparation of the Ti<sub>13</sub>·6THF cluster can be found in Ref. 3. Approximately 2 g of material were filled into a stainless-steel reactor suitable for kinetic measurements (see Ref. 3). A modified Sieverts apparatus was used for the kinetic measurements. Experiments were performed either at a constant heating rate or under isothermal conditions. Prior to the kinetic measurements, the material was cycled until a reasonably stable kinetic state was reached for desorption. At constant heating rate of 0.5 K/min, this was accomplished only after 12 sorption cycles. This paper therefore presents the data from cycle 13 onwards. After these many cycles, the oxidation state and the local environment of Ti have reached a stable state independent of the initial kind of the Ti doping (e.g., TiCl<sub>3</sub>, Ti<sub>13</sub>·6THF, etc.).<sup>16</sup> Absorption was performed at gas pressures of 90 bar at 100 °C, desorption against a calibrated reference volume in which the pressure increased from 10<sup>-3</sup> bar to ≈0.5 bar H<sub>2</sub> (D<sub>2</sub>) during the experiment. A description of the experimental setup can be found elsewhere.<sup>12</sup> After the hydrogen cycles, the gas was replaced by deuterium. After two reabsorptions of the sample with deuterium, the same set of kinetic measurements were repeated with NaAlD<sub>4</sub>. Although the powder is only desorbed to NaH as the final state [see Eq. (2)], the isotope exchange from H to D

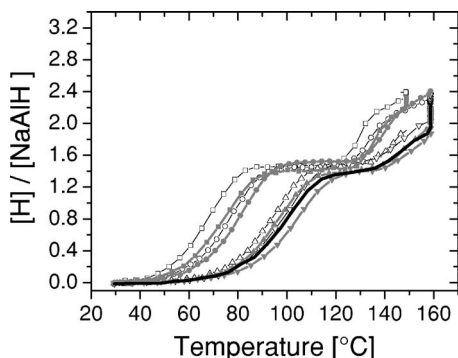


FIG. 1. Hydrogen (open symbols) and deuterium desorption (solid symbols) of  $\text{NaAlH}_4$  doped with 5 mol %  $\text{Ti}_{13}\cdot 6\text{THF}$  at various heating rates [0.04 K/min ( $\square$ ,  $\blacksquare$ ), 0.1 K/min ( $\circ$ ,  $\bullet$ ), 0.5 K/min ( $\triangle$ ,  $\blacktriangle$ ), and 0.8 K/min ( $\nabla$ ,  $\blacktriangledown$ )]. The solid line stands for hydrogen desorption with  $\beta=0.8$  K/min after the final deuterium run and one subsequent hydrogen absorption.

was found to be almost complete after two cycles, presumably because that the gas exchange is much faster than the desorption and/or absorption kinetics.<sup>10</sup> It should be noted that neither the sample nor the heating system of the reactor had been altered when the gases were changed. The experimental conditions were identical for the hydrogen and deuterium cycles.

### III. RESULTS

Figure 1 shows the amount of desorbed  $\text{H}_2$  (open symbols) or  $\text{D}_2$  (solid symbols) of Ti-doped  $\text{NaAlH}_4$  as a function of temperature for various heating rates  $\beta$  between 0.04 and 0.8 K/min. The two desorption steps [see Eqs. (1) and (2)] are clearly visible as the temperature of the sample rises. During cycling, the reversible storage capacity remains constant at 2.4  $[\text{H}]/[\text{NaAlH}_4]$  which corresponds to  $\approx 4.5$  wt %. For high heating rates, decomposition was still incomplete when the maximum temperature was reached. In this case, the reactor was kept isothermally at maximum temperature until desorption had been completed.

As expected, the storage capacities of the deuterated and hydrogenated samples are identical. However, the reaction rates were found to differ. The desorption curves of the deuterate consistently are shifted towards higher temperatures, compared to the hydrogenated sample. To exclude other effects (e.g., deterioration of the powder), we repeated a run with hydrogen ( $\beta=0.8$  K/min) after the final deuterium cycle (Fig. 1, solid line). The curve does not fully coincide with the run measured many cycles earlier. In principle, it could be that the hydrogen-deuterium exchange had not been complete in only one reabsorption run. Another possibility is aging of the sample during the experiment. This last measurement can, thus, be taken as the upper limit for aging effects which obviously are much smaller than the shift in temperature observed when hydrogen is replaced by deuterium.

Moreover, the reaction rate was studied under isothermal conditions (see Fig. 2). Successive runs with hydrogen (cycle 23, solid line), deuterium (cycle 24, dashed line), and again

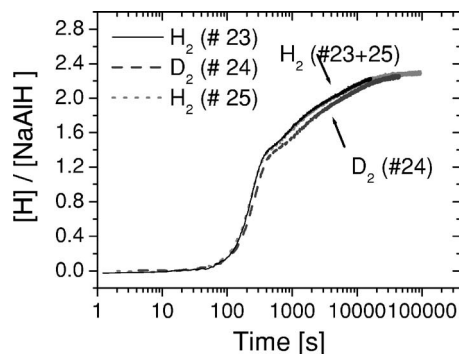


FIG. 2. Subsequent isothermal desorptions at  $T=150$  °C for hydrogen (cycle 23), deuterium (cycle 24), and hydrogen (cycle 25).

with hydrogen (cycle 25, dotted line) are shown. The data confirm the small, but significant difference in kinetics that is observed when hydrogen is replaced by deuterium: hydrogen cycles 23 and 25 coincide, whereas cycle 24 (deuterium) is delayed. That cycles 23 and 25 are identical supports the assumption that the isotope exchange is almost complete after only one reabsorption cycle.

Figure 3 shows isothermal hydrogen and deuterium absorption as a function of time. The sample was kept under isothermal conditions at 100 °C. For the first absorption step from  $\text{NaH}$  to  $\text{Na}_3\text{AlH}_6$  [i.e., the reverse reaction of Eq. (2)], a pressure of  $\approx 23$  bar  $\text{H}_2$  or  $\text{D}_2$  was applied. The reaction from  $\text{Na}_3\text{AlH}_6$  to  $\text{NaAlH}_4$  was performed at  $\approx 91$  bar gas pressure. For both reaction steps, the gas uptake (and subsequent phase transition) is slower in the case of deuterium. Moreover, the initial temperature increase measured in the powder bed is larger in the case of hydrogen (see Fig. 4). If the thermal heat conductivities of  $\text{NaAl}(\text{H},\text{D})_4$ ,  $\text{Na}_3\text{Al}(\text{H},\text{D})_6$ , and  $\text{Na}(\text{H},\text{D})$  roughly correspond to the values of the gas species used, the hydrogenated sample should dissipate the heat generated during exothermal uptake faster than the deuteride. Hence, a smaller temperature rise is expected for hydrogen. That the opposite is observed, i.e., a smaller temperature increase when  $\text{D}_2$  is introduced, thus is a clear indication of a lower  $\text{D}_2$  reaction rate in both reaction steps.

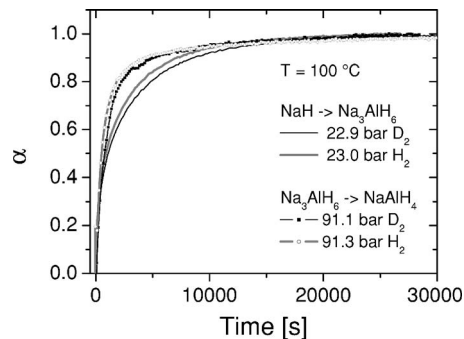


FIG. 3. Normalized isothermal absorption  $\alpha$  at  $T=100$  °C at applied gas pressures of 23 bar ( $\text{NaH} \rightarrow \text{Na}_3\text{AlH}_6$ ) and 91 bar ( $\text{Na}_3\text{AlH}_6 \rightarrow \text{NaAlH}_4$ ), respectively.

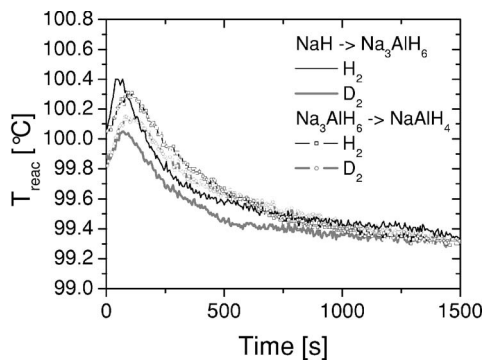
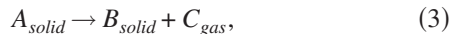


FIG. 4. Temperature inside the powder bed during the first  $\approx 1000$  s of absorption of hydrogen (black) or deuterium (gray).

#### IV. DISCUSSION

In a solid-state reaction,



the reaction rate at isothermal conditions generally can be described by

$$\frac{d\alpha}{dt} = k(T)f(\alpha), \quad (4)$$

where  $\alpha$  is the normalized fraction of the material converted,  $k$  is the reaction-rate constant,  $t$  is the time, and  $f(\alpha)$  describes the reaction model. As a function of the rate limiting step (e.g., surface processes, diffusion limited conversions, etc.),  $f(\alpha)$  takes various functional forms<sup>17</sup> while, in a simple approach, it only depends on the amount of material,  $\alpha$ , already converted. The temperature dependence of the reaction rate is taken into account in the rate constant usually described by an Arrhenius expression:

$$k(T) = k_0 \exp\left(\frac{-E_a}{RT}\right), \quad (5)$$

where  $k_0$  is the temperature-independent rate constant,  $E_a$  is the activation energy,  $R$  is the molar gas constant, and  $T$  is the temperature.

##### A. Desorption

For experiments which are nonisothermal but are run at a constant heating rate  $\beta$ , with

$$T = \beta t + T_0, \quad (6)$$

a range of methods have been developed to determine the activation energy, which rely on the measurement of the temperature at which a fixed fraction  $\alpha$  of the new phase is generated (isoconversion methods).<sup>18</sup> These include the generalized Kissinger or Kissinger-Akahira-Sunrose (KAS) approximation:

$$\ln\left(\frac{\beta}{T^2}\right) \sim \frac{-E_a}{RT}, \quad (7)$$

and a plot of  $\ln(\beta/T^2)$  vs  $1/T$  for fixed  $\alpha$  and various heating rates  $\beta$  yields a straight line with the slope of  $-E_a/R$ . Alter-

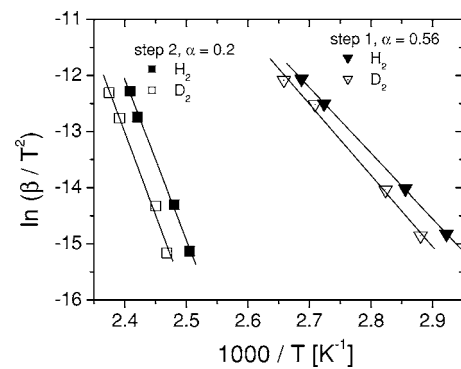


FIG. 5. KAS analysis for the decomposition of  $\text{NaAlH}_4$  to  $\text{Na}_3\text{AlH}_6$  (at  $\alpha=0.56$ ), and  $\text{Na}_3\text{AlH}_6$  to  $\text{NaH}$  (+Al) (at  $\alpha=0.2$ ), for hydrogen (solid symbols) and deuterium cycles (open symbols).

natively, the temperature at the maximum conversion rate,  $T_p$ , with  $\left.\frac{d\alpha}{dt}\right|_{T_p} = \max$  can be used in Eq. (7) (Kissinger plot). The isoconversion methods have the advantage of being independent of the assumptions made for the reaction model. Hence  $E_a$  can be determined without any detailed knowledge of the reaction mechanism. Of course, the applied hydrogen pressure is a crucial factor for hydrogen release and uptake. In our hydrogen/deuterium exchange experiments, backpressure was the same in both types of experiment. Therefore, we assume that the pressure has no influence on the comparison of reaction rates. The validity of this approach will be justified below.

In Fig. 5,  $\ln(\beta/T^2)$  vs  $1/T$  is plotted for hydrogen ( $\blacktriangledown$ ) and deuterium ( $\nabla$ ) desorption at  $\alpha=0.56$  ( $\text{NaAlH}_4 \rightarrow \text{Na}_3\text{AlH}_6$ ) as an example. Evaluation of the slopes (for various  $\alpha$ ) yields an average value  $E_a=95.0 \pm 2$  kJ/mol for  $\text{H}_2$  desorption and  $E_a=102 \pm 2.3$  kJ/mol for  $\text{D}_2$  desorption. Similar values are obtained from a Kissinger analysis at maximum conversion rate:  $E_a$  amounts to 92.1 kJ/mol for  $\text{H}_2$  and to 101.6 kJ/mol for  $\text{D}_2$ . These values agree with data previously published by the authors,<sup>19</sup> but they are slightly higher than the data published in Ref. 20. For the decomposition step  $\text{Na}_3\text{AlH}_6 \rightarrow \text{NaH}$ ,  $E_{a2}$  varies continuously with the amount of material converted. In the accessible range,  $0.15 \leq \alpha \leq 0.45$  (due to incomplete desorption at high heating rates),  $E_{a2}$  decreases from 260 to  $\sim 176$  kJ/mol. However, there is no systematic variation of  $E_{a2}$  as a function of hydrogen or deuterium desorption. The data for  $\alpha=0.2$  are shown as an example in Fig. 5. This contrasts with the first decomposition step where, under the chosen experimental conditions,  $E_a$  depends on the gas species used. Nevertheless, the intercept with the y axis in the KAS analysis differs for  $\text{H}_2$  and  $\text{D}_2$ , indicating that the prefactor is isotope dependent, whereas  $E_a$  possibly is the same for hydrogen and deuterium in the second desorption step.

It has been argued before that hydrogen desorption in alanes follows a nucleation and growth process and, hence, can best be described in a Johnson-Mehl-Avrami (JMA) based model.<sup>3,11-13</sup> The reaction-rate function  $f(\alpha)$  for isothermal conditions then takes the functional form<sup>21</sup> of

$$f(\alpha) = n(1 - \alpha)[- \ln(1 - \alpha)]^{(n-1)/n}, \quad (8)$$

where the Avrami exponent  $n$  is a geometry factor describing the dimensionality of the growing phase. Equations (8) and (4) after integration yield

$$\alpha = 1 - \exp[-(kt)^n]. \quad (9)$$

For linear heating conditions, this furnishes<sup>21,22</sup>

$$\ln\left(\frac{T_p^2}{\beta}\right) + \ln\left(\frac{k_0 R}{E_a}\right) - \left(\frac{E_a}{RT_p}\right) \approx \frac{2RT_p}{E_a} \left[1 - \frac{1}{n^2}\right], \quad (10)$$

where, for the temperature range and heating rates considered, the term on the right is negligible compared to the individual terms on the left. Again, a plot of  $\ln(T_p^2/\beta)$  vs  $1/T_p$  furnishes the activation energy, and  $n$  is given by<sup>22</sup>

$$n = \frac{d\alpha}{dt} \bigg|_p RT_p^2 (0.37\beta E_a)^{-1}. \quad (11)$$

From this analysis, we obtain  $n=1.01$  ( $H_2$ ) and  $n=0.93$  ( $D_2$ ), respectively, for the decomposition of  $NaAlH_4$  to  $Na_3AlH_6$ . This indicates a diffusion-limited process as suggested<sup>3,13</sup> previously with site saturation of the nuclei or a phase transformation rate limiting step at the interface.<sup>23</sup> During desorption of  $NaAlH_4$  into  $Na_3AlH_6$ , the reaction rate will be determined by one of the following steps: Initially, the Al-H bond has to break up. Subsequently, hydrogen will be transported to the surface to recombine and desorb. Furthermore, in the remaining host material, the two phases,  $Na_3AlH_6$  and Al, emerge. Hence the lattice has to be rearranged and large-scale mass transport will occur. The kinetic isotope effect observed indicates that the rate limiting step for  $NaAlH_4$  decomposition into  $Na_3AlH_6$  involves a hydrogen-containing species. For hydrogen-bond breaking or atomic hydrogen diffusion through the lattice, the ratio of the apparent activation energies is expected to be  $\sqrt{m_H}/\sqrt{m_D}=0.707$ , where  $m_{H,D}$  are the masses of hydrogen and deuterium, respectively. This is clearly lower than the ratio of 0.93 obtained experimentally. However, if  $AlH_3$  ( $m_{AlH_3}=30$  amu) or  $NaH$  ( $m_{NaH}=24$  amu) is assumed to be mobile species, the  $\sqrt{m_H}/\sqrt{m_D}$  ratio equals 0.95 and 0.98, respectively, which is considerably closer to the experimental value.

### B. Absorption

Under isothermal conditions, the Arrhenius factor is constant and Eq. (9) can be rewritten as

$$\ln[-\ln(1 - \alpha)] = n \ln t + n \ln k. \quad (12)$$

In Fig. 6, the absorption data are replotted as  $\ln[-\ln(1 - \alpha)]$  vs  $\ln t$ ; the slope of this plot yields the Avrami coefficient,  $n$ . For  $NaH (+Al) \rightarrow Na_3AlH_6$ ,  $n=0.62$  for hydrogen absorption and 0.60 for deuterium absorption. The Avrami exponent indicates a diffusion-limited process with a constant number of nuclei. From the intercepts, it is  $\ln k = -7.484$  ( $H_2$ ) and  $\ln k = -7.650$  ( $D_2$ ) which result in a prefactor ratio  $k_H/k_D = 1.18$ . In the JMA equation, the prefactor includes the activation energy in the shape of the Arrhenius term and the diffusion constant,  $D_0$ .<sup>21</sup> However, they cannot be separated

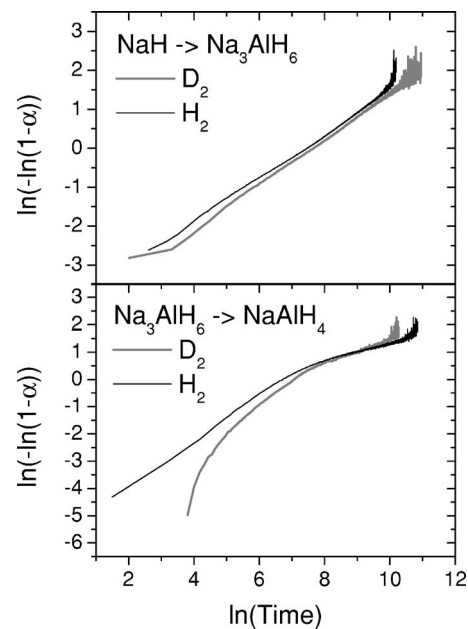


FIG. 6.  $\ln[-\ln(1 - \alpha)]$  vs  $\ln t$  for absorption step 1,  $NaH \rightarrow Na_3AlH_6$  (upper panel), and step 2,  $Na_3AlH_6 \rightarrow NaAlH_4$ .

from measurements taken at a single temperature. Let us suppose that  $k_{H,D}$  can be described by

$$k_x = AD_x \exp\left(\frac{-E_{a,x}}{RT}\right), \quad (13)$$

where  $D_x$  and  $E_{a,x}$  denote the diffusion coefficient and activation energy for  $x=H$  or  $D$ , and  $A$  takes into account all isotope-independent and thus constant factors. For the ratio,  $\frac{k_H}{k_D}$ , it holds that

$$\begin{aligned} R_{iso} &= \frac{k_H}{k_D} \\ &= \frac{D_H \exp\left(\frac{-E_H}{RT}\right)}{D_D \exp\left(\frac{-E_D}{RT}\right)} \\ &= \sqrt{\frac{m_D}{m_H}} \exp\left[\frac{-E_{a,H}}{RT} \left(1 - \sqrt{\frac{m_D}{m_H}}\right)\right], \end{aligned} \quad (14)$$

where, for the second part, we assumed the isotope dependence discussed above. The exponential factor of Eq. (14) explicitly contains the apparent activation energies. For typical values obtained for reabsorption, this factor will dominate  $R_{iso}$ , except for  $\sqrt{\frac{m_D}{m_H}}$  close to unity. In order to allow for the very low experimental ratio, masses should not differ by more than 1%–2% (with  $E_{a,H}=56.2$  kJ/mol, Ref. 20). This confirms that the apparent activation energies do not reflect atomic hydrogen diffusion, matching the authors observation of the reversed reaction, i.e., desorption step 2, where no significant isotope dependence of the activation energy was found.

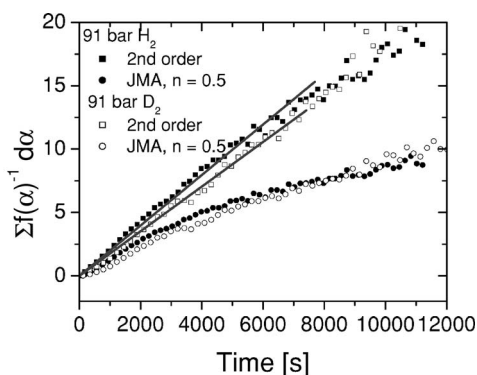


FIG. 7. Plot of the absorption data  $\text{Na}_3\text{AlH}_6 \rightarrow \text{NaAlH}_4$  recalculated according Eq. (15) to test the reaction models. Results are shown for a second-order reaction and a JMA model with  $n=0.5$  (see text).

The second reaction step, starting from  $\text{Na}_3\text{AlH}_6$  to produce  $\text{NaAlH}_4$ , is not unambiguously classified by the JMA analysis. A plot according to Eq. (12) shows two distinct slopes, as if the reaction mechanism changed during absorption (see Fig. 6). Likewise, the reaction model best describing the reaction is not defined clearly: Eq. (4) can be rewritten as

$$\frac{\int f(\alpha)^{-1} d\alpha}{\exp\left(\frac{-E_a}{RT}\right)} = k_0 t. \quad (15)$$

At constant  $T$ , a plot of the right-hand side vs  $t$  should result in a straight line with a positive slope  $k_0$ . Several reaction models were tested (see Ref. 17). Both a second-order reaction with  $f(\alpha)=(1-\alpha)^2$  and a JMA model with  $n=0.5$  seem possible. In Fig. 7, both models are compared for the data indicated in Fig. 3. For  $t \leq 10\,000$  s, a second-order reaction model is favored. This is independent of the gas species used, i.e., the reaction mechanism is independent of hydrogen/deuterium exchange, while the slope is a factor of 1.13 larger for  $\text{H}_2$  absorption than for the  $\text{D}_2$  case. As discussed above for the reabsorption of  $\text{NaH}$  to  $\text{Na}_3\text{AlH}_6$ , this indicates a ratio of activation energies close to unity.

### C. Thermodynamics of hydrogen/deuterium exchange

In the experiments discussed above, a small but significant difference was found in the kinetic parameters of hydrogen and deuterium cycling of Ti-doped  $\text{NaAlH}_4$ . In order to exclude any effect possibly stemming from a difference in the reaction enthalpy,  $\Delta H$ , pressure-composition isotherms (in desorption) were determined for  $\text{NaAlH}_4$  and  $\text{NaAlD}_4$ . For  $\text{LiAlH}_4$ , a small difference in  $\Delta H$  was predicted theoretically,<sup>24</sup> i.e., the deuteride is supposed to be slightly more stable. Figure 8 shows the isotherms obtained at  $T=130$  °C (desorption). The temperature was chosen as a compromise so as to minimize deterioration and a reaction rate allowing the equilibrium to be reached within a reasonable time. A new pressure was set for each point, and subse-

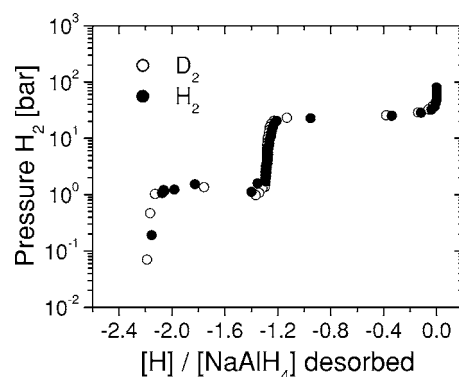


FIG. 8. Pressure-composition isotherms ( $T=130$  °C, in desorption) for Ti-doped  $\text{NaAlH}_4$  (●) and  $\text{NaAlD}_4$  (○).

quently, the system was permitted to reach equilibrium. Apparently, the plateau pressures measured for hydrogen and deuterium decomposition at 130 °C are identical within experimental limits of error. Hence, the thermodynamic driving force for hydrogen and deuterium loading and unloading is expected to be the same.

The reaction rate will depend on the pressure applied  $p_{app}$  and the plateau pressure  $p_{eq}$  at temperature  $T$  according to  $\ln \frac{p_{app}}{p_{eq}}$ .<sup>20</sup> Using the values for  $p_{eq}$  obtained at 130 °C and the experimental pressure conditions, the variation of this factor is estimated to be negligible during absorption (reaction steps 1 and 2) and during decomposition of  $\text{NaAlH}_4$  to  $\text{Na}_3\text{AlH}_6$ . However, during the second desorption step in the linear heating experiments, i.e., the decomposition of  $\text{Na}_3\text{AlH}_6$ ,  $p_{app}$  and  $p_{eq}$  are of the same order of magnitude and the factor of  $\ln \frac{p_{app}}{p_{eq}}$  varies considerably during the experiment due to the temperature dependence of  $p_{eq}$ . Probably, this is the reason for the decreasing activation energy,  $E_{a2}$ , with increasing fraction,  $\alpha$ , as observed in the KAS analysis. For all other cases, the pressure-composition isotherm measurements confirm earlier assumptions on the analysis of the kinetic data.

## V. CONCLUSIONS

In their experiments, the authors found a small but significant difference in the kinetic parameters of hydrogen and deuterium uptake and release in Ti-doped  $\text{NaAlH}_4$ . While evaluation of the Avrami coefficients indicates the reaction processes to be unchanged by the isotope exchange, the kinetic parameters are altered. For the decomposition of  $\text{NaAlH}_4$  to  $\text{Na}_3\text{AlH}_6$ , the ratio of activation energies amounts to  $\approx 0.93$ . This value suggests that atomic hydrogen is not the rate-controlling unit, but diffusion of a heavier species, such as  $\text{Al}_x\text{H}_y$  or  $\text{NaH}$ , seems to be likely. For the other reaction steps, i.e., desorption of the hexahydride and the two reabsorption reactions, it is proposed that the ratio of activation energies must be close to unity, although the reaction rates exhibit isotope dependency. Again, this excludes a dominant contribution from atomic hydrogen. It rather indicates a reaction rate controlled by hydrogen-containing species of higher mass.

\*Electronic address: lohstroh@int.fzk.de

- <sup>1</sup>B. Bogdanović and M. Schwickardi, *J. Alloys Compd.* **253**, 1 (1997).
- <sup>2</sup>F. Schüth, B. Bogdanović, and M. Felderhoff, *Chem. Commun. (Cambridge)* **2004**, 2249.
- <sup>3</sup>M. Fichtner, O. Fuhr, O. Kircher, and J. Rothe, *Nanotechnology* **14**, 778 (2003).
- <sup>4</sup>M. Fichtner, *Adv. Eng. Mater.* **7**, 443 (2005).
- <sup>5</sup>S. Orimo, Y. Nakamori, G. Kitahara, N. Ohba, S. Towata, and A. Züttel, *J. Alloys Compd.* **404**, 427 (2005).
- <sup>6</sup>F. E. Pinkerton, G. P. Meisner, M. S. Meyer, M. P. Balogh, and M. D. Kundrat, *J. Phys. Chem. B* **109**, 6 (2005).
- <sup>7</sup>Y. E. Filinchuk, K. Yvon, G. P. Meisner, F. E. Pinkerton, and M. P. Balogh, *Inorg. Chem.* **45**, 1433 (2006).
- <sup>8</sup>G. P. Meisner, M. L. Scullin, M. P. Balogh, F. E. Pinkerton, and M. S. Meyer, *J. Phys. Chem. B* **110**, 4186 (2006).
- <sup>9</sup>J. J. Vajo, F. Mertens, C. C. Ahn, R. C. Bowman, and B. Fultz, *J. Phys. Chem. B* **108**, 13977 (2004).
- <sup>10</sup>J. M. Bellosta von Colbe, W. Schmidt, M. Felderhoff, B. Bogdanović, and F. Schüth, *Angew. Chem., Int. Ed.* **45**, 3663 (2006).
- <sup>11</sup>D. Blanchard, H. W. Brinks, and B. C. Hauback, *J. Alloys Compd.* **416**, 72 (2006).
- <sup>12</sup>O. Kircher and M. Fichtner, *J. Appl. Phys.* **95**, 7748 (2004).
- <sup>13</sup>A. Andreasen, T. Vegge, and A. S. Pedersen, *J. Solid State Chem.* **178**, 3664 (2005).
- <sup>14</sup>K. J. Gross, S. Guthrie, S. Takara, and G. Thomas, *J. Alloys Compd.* **297**, 270 (2000).
- <sup>15</sup>Q. J. Fu, A. J. Ramirez-Cuesta, and S. C. Tsang, *J. Phys. Chem. B* **110**, 711 (2006).
- <sup>16</sup>A. Leon, O. Kircher, M. Fichtner, J. Rothe, and D. Schild, *J. Phys. Chem. B* **110**, 1192 (2006).
- <sup>17</sup>A. Khawan and D. Flanagan, *Thermochim. Acta* **429**, 93 (2005).
- <sup>18</sup>M. J. Starink, *Thermochim. Acta* **404**, 163 (2003).
- <sup>19</sup>O. Kircher and M. Fichtner, *J. Alloys Compd.* **404**, 339 (2005).
- <sup>20</sup>W. Luo and K. J. Gross, *J. Alloys Compd.* **385**, 224 (2004).
- <sup>21</sup>G. Ruitenberg, E. Woldt, and A. K. Petford-Long, *Thermochim. Acta* **378**, 97 (2001).
- <sup>22</sup>J. Vázquez, D. García, P. L. López-Aleman, P. Villares, and R. Jiménez-Garay, *Thermochim. Acta* **430**, 173 (2005).
- <sup>23</sup>P. S. Rudman, *J. Less-Common Met.* **89**, 93 (1983).
- <sup>24</sup>T. J. Frankcombe and G.-J. Kroes, *Chem. Phys. Lett.* **423**, 102 (2005).